Overdominant effect of a *CHRNA4* polymorphism on cingulo-opercular network activity and cognitive control

Abbreviated Title: Neuroimaging genetics of *CHRNA4*

Sepideh Sadaghiani* [1,2,3], Bernard Ng[1,4], Andre Altmann[1,5], Jean-Baptiste Poline[6], Tobias Banaschewski[7]; Arun L.W. Bokde[8]; Uli Bromberg[9]; Christian Büchel[9]; Erin Burke Quinlan[10]; Patricia Conrod[10]; Sylvane Desrivières[10]; Herta Flor[11,12]; Vincent Frouin[13]; Hugh Garavan[14]; Penny Gowland[15]; Jürgen Gallinat[16], Andreas Heinz[16]; Bernd Ittermann[17]; Jean-Luc Martinot[18], Marie-Laure Paillère Martinot[19]; Hervé Lemaitre[19]; Frauke Nees[7,11]; Dimitri Papadopoulos Orfanos[13]; Tomáš Paus[20]; Luise Poustka[21,22], Sabina Millenet[7]; Juliane H. Fröhner[23]; Michael N. Smolka[23]; Henrik Walter[16]; Robert Whelan[24]; Gunter Schumann[10], Valerio Napolioni[1], Michael Greicius[1]

[1] Department of Neurology and Neurological Sciences, Stanford University, Stanford, CA 94305, USA
[2] Department of Psychology, University of Illinois at Urbana-Champaign, Urbana, IL 61801, USA
[3] Beckman Institute for Advanced Science and Technology, Urbana, IL 61801, USA
[4] Department of Statistics, University of British Columbia, Vancouver, BC V6T 1Z4, Canada
[5] Translational Imaging Group, Centre for Medical Image Computing (CMIC), Department of Medical Physics & Bioengineering, University College London, London WC1E 6BT, United Kingdom
[6] Department of Psychology, University of California at Berkeley, Berkeley, CA 94720, USA
[7] Department of Child and Adolescent Psychiatry and Psychotherapy, Central Institute of Mental Health, Medical Faculty Mannheim, Heidelberg University, 68159 Mannheim, Germany;
[8] Discipline of Psychiatry, School of Medicine and Trinity College Institute of Neuroscience, Trinity College Dublin, Dublin, Ireland;
[9] University Medical Centre Hamburg-Eppendorf, 20246, Hamburg, Germany;
[10] Medical Research Council - Social, Genetic and Developmental Psychiatry Centre, Institute of Psychiatry, Psychology & Neuroscience, King's College London, United Kingdom;
[11] Department of Cognitive and Clinical Neuroscience, Central Institute of Mental Health, Medical Faculty Mannheim, Heidelberg University, 68159 Mannheim, Germany;
[12] Department of Psychology, School of Social Sciences, University of Mannheim, 68131 Mannheim, Germany;
[13] NeuroSpin, CEA, Université Paris-Saclay, F-91191 Gif-sur-Yvette, France;
[14] Departments of Psychiatry and Psychology, University of Vermont, 05405 Burlington, Vermont, USA;
[15] Sir Peter Mansfield Imaging Centre School of Physics and Astronomy, University of Nottingham, University Park, Nottingham, United Kingdom;
[16] Department of Psychiatry and Psychotherapy, Campus Charité Mitte, Charité, Universitätsmedizin Berlin, Berlin, Germany;
[17] Physikalisch-Technische Bundesanstalt (PTB), Berlin, Germany
[18] Institut National de la Santé et de la Recherche Médicale, INSERM Unit 1000 "Neuroimaging & Psychiatry", University Paris Sud – Paris Saclay, University Paris Descartes; Service Hospitalier Frédéric Joliot, Orsay; and Maison de Solenn, Paris, France
[19] Institut National de la Santé et de la Recherche Médicale, INSERM Unit 1000 "Neuroimaging & Psychiatry", University Paris Sud – Paris Saclay, University Paris Descartes; and AP-HP, Department of Adolescent Psychopathology and Medicine, Maison de Solenn, Cochin Hospital, Paris, France
[20] Rotman Research Institute, Baycrest and Departments of Psychology and Psychiatry, University of Toronto, Toronto, Ontario, M6A 2E1, Canada;
[21] Department of Child and Adolescent Psychiatry and Psychotherapy, University Medical Centre Göttingen, 37075 Göttingen, Germany;
[22] Clinic for Child and Adolescent Psychiatry, Medical University of Vienna, 1090 Vienna, Austria;
[23] Department of Psychiatry and Neuroimaging Center, Technische Universität Dresden, Dresden, Germany;
[24] School of Psychology and Global Brain Health Institute, Trinity College Dublin, Ireland;

* corresponding author: Sepideh Sadaghiani, PhD, Assistant Professor
Department of Psychology, Cognitive Neuroscience Division
Beckman Institute for Advanced Science and Technology
University of Illinois at Urbana-Champaign
Beckman Institute, 405 N Mathews Avenue
Urbana, IL 61801
Sepideh@illinois.edu
https://connectlab.beckman.illinois.edu

Number of pages: 23, **Number of figures**: 4, **Number of tables**: 2, No multimedia or models
Number of words: Abstract: 250, Introduction: 659, Discussion: 1409

Conflict of Interest: Dr. Banaschewski has served as an advisor or consultant to Bristol-Myers Squibb, Desitin Arzneimittel, Eli Lilly, Medice, Novartis, Pfizer, Shire, UCB, and Vifor Pharma; he has received conference attendance support, conference support, or speaking fees from Eli Lilly, Janssen McNeil, Medice, Novartis, Shire, and UCB; and he is involved in clinical trials conducted by Eli Lilly, Novartis, and Shire; the present work is unrelated to these relationships.
Dr. Barker has received funding for a PhD student and honoraria for teaching on scanner programming courses from General Electric Healthcare; he acts as a consultant for IXICO.
Dr. Walter received a speaker honorarium from Servier (2014). The other authors report no biomedical financial interests or potential conflicts of interest.

Acknowledgments: We thank Stephen M. Malone for supporting us in a multi-modal investigation of *CHRNA4*. This work was supported by funding from The Feldman Family Foundation and The J. W. Bagley Foundation. AA holds an MRC eMedLab Medical Bioinformatics Career Development Fellowship. This work was supported by the Medical Research Council [grant number MR/L016311/1].
The IMAGEN consortium has received support from the following sources: the European Union-funded FP6 Integrated Project IMAGEN (Reinforcement-related behaviour in normal brain function and psychopathology) (LSHM-CT- 2007-037286), the Horizon 2020 funded ERC Advanced Grant 'STRATIFY' (Brain network based stratification of reinforcement-related disorders) (695313), ERANID (Understanding the Interplay between Cultural, Biological and Subjective Factors in Drug Use Pathways) (PR-ST-0416-10004), BRIDGET (JPND: BRain Imaging, cognition Dementia and next generation GEnomics) (MR/N027558/1), the FP7 projects IMAGEMEND(602450; IMAging GEnetics for MENtal Disorders) and MATRICS (603016), the Innovative Medicine Initiative Project EU-AIMS (115300-2), the Medical Research Council Grant 'c-VEDA' (Consortium on Vulnerability to Externalizing Disorders and Addictions) (MR/N000390/1), the Swedish Research Council FORMAS, the Medical Research Council, the National Institute for Health Research (NIHR) Biomedical Research Centre at South London and Maudsley NHS Foundation Trust and King's College London, the Bundesministeriumfür Bildung und Forschung (BMBF grants 01GS08152; 01EV0711; eMED SysAlc01ZX1311A; Forschungsnetz AERIAL), the Deutsche Forschungsgemeinschaft (DFG grants SM 80/7-1, SM 80/7-2, SFB 940/1). Further support was provided by grants from: ANR (project AF12-NEUR0008-01 - WM2NA, and ANR-12-SAMA-0004), the Fondation de France, the Fondation pour la Recherche Médicale, the Mission Interministérielle de Lutte-contre-les-Drogues-et-les-Conduites-Addictives (MILDECA), the Assistance-Publique-Hôpitaux-de-Paris and INSERM (interface grant), Paris Sud University IDEX 2012; the National Institutes of Health, Science Foundation Ireland (16/ERCD/3797), U.S.A. (Axon, Testosterone and Mental Health during

Adolescence; RO1 MH085772-01A1), and by NIH Consortium grant U54 EB020403, supported by a cross-NIH alliance that funds Big Data to Knowledge Centres of Excellence.

Abstract

The nicotinic system plays an important role in cognitive control, and is implicated in several neuropsychiatric conditions. Yet, the contributions of genetic variability in this system to individuals' cognitive control abilities are poorly understood, and the brain processes that mediate such genetic contributions remain largely unidentified. In this first large-scale neuroimaging genetics study of the human nicotinic receptor system (two cohorts, males and females, fMRI total N=1586, behavioral total N=3650), we investigated a common polymorphism of the high-affinity nicotinic receptor α4β2 (rs1044396 on the *CHRNA4* gene) previously implicated in behavioral and nicotine-related studies (albeit with inconsistent major/minor allele impacts). Based on our prior neuroimaging findings, we expected this polymorphism to impact neural activity in the cingulo-opercular network involved in core cognitive control processes including maintenance of alertness. Consistent across the cohorts, all cortical areas of the cingulo-opercular network showed higher activity in heterozygotes compared to both types of homozygotes during cognitive engagement. This inverted U-shaped relation reflects an overdominant effect, i.e. allelic interaction (cumulative evidence $p=1.33*10^{-5}$). Furthermore, heterozygotes performed more accurately in behavioral tasks that primarily depend on sustained alertness. No effects were observed for haplotypes of the surrounding *CHRNA4* region, supporting a true overdominant effect at rs1044396. As a possible mechanism, we observed that this polymorphism is an expression quantitative trait locus (eQTL) modulating *CHRNA4* expression levels. This is the first report of overdominance in the nicotinic system. These findings connect *CHRNA4* genotype, cingulo-opercular network activation and sustained alertness, providing insights into how genetics shapes individuals' cognitive control abilities.

Significance Statement:

The nicotinic acetylcholine system plays a central role in neuromodulatory regulation of cognitive control processes, and is dysregulated in several neuropsychiatric disorders. In spite of this functional importance, no large-scale neuroimaging genetics studies have targeted the contributions of genetic variability in this system to human brain activity. Here, we show impact of a common polymorphism of the high-affinity nicotinic receptor α4β2, consistent across brain activity and behavior in two large human cohorts. We report a hitherto unknown overdominant effect (allelic interaction) at this locus, where the heterozygotes show higher activity in the cingulo-opercular network underlying alertness maintenance, and higher behavioral alertness

performance than both homozygous groups. This gene-brain-behavior relationship informs about the biological basis of inter-individual differences in cognitive control.

Introduction

Cognitive control abilities are central to all goal-directed behavior but vary widely across individuals (Gruszka et al., 2010; Mennes et al., 2011). While cognitive control capacities have strong heritable components (Friedman et al., 2008; Chang et al., 2013), it is largely unknown through which brain mechanisms genetic variability translates into their inter-individual differences. Neuromodulatory neurotransmitter systems are central to cognitive control given their capacity to broadly modify signal processing across large areas of the brain. In particular, the broad acetylcholinergic innervation of the neocortex originating in the basal forebrain plays a central role in cognitive control, especially tonic control functions (Knott et al., 1999; Kozak et al., 2006). Both tonic control functions and acetylcholinergic modulation are dysregulated in several neuropsychiatric disorders (Lesh et al., 2011; Sarter and Paolone, 2011; Higley and Picciotto, 2014), reward processing and addiction to various substances (Hendrickson et al., 2013). Yet, how genetic polymorphisms in this modulatory system influence brain function is poorly understood.

The most abundant high-affinity nAChR in the mammalian brain is the α4β2 receptor (Albuquerque et al., 2009). Among the single nucleotide polymorphisms (SNPs) of the underlying genes *CHRNA4* and *CHRNB2*, rs1044396 (NM_000744.6:c.1629C>T) of the α4 subunit (chromosome 20q13.3) has been implicated in behaviorally relevant contexts, albeit with inconsistent impact from major/minor alleles. While this SNP itself is synonymous (NP_000735.1:p.Ser543=), it is part of a functional *CHRNA4* haplotype affecting receptor sensitivity to acetylcholine (Eggert et al., 2015). The SNP is implicated in nicotine consumption and addiction (Feng et al., 2004; Breitling et al., 2009), as well as phasic cognitive control functions. However, this cognitive literature (often comprising relatively small sample sizes) is inconclusive, since some studies report behavioral advantage of the rs1044396-T allele (Greenwood et al., 2012, 2005; Espeseth et al., 2010), and some of the rs1044396-C allele (Parasuraman et al., 2005; Reinvang et al., 2009). Furthermore, the brain mechanisms mediating the impact on behavior are largely unknown. The only two neuroimaging investigations of rs1044396 have been carried out in relatively small sample sizes N<50, and one study lacks heterozygous participants (Winterer et al., 2007; Gießing et al., 2012).

The cortical target regions of acetylcholinergic stimulation may shed light on the underlying pathway from genetic variability to cognitive abilities. Using positron emission tomography, we found that across the cerebral cortex α4β2 receptor density was highest bilaterally in the dorsal anterior cingulate cortex and anterior insula (Picard et al., 2013). Together with the thalamus, the brain region with the highest nAchR density (Gallezot et al., 2005), these areas constitute the core of the cingulo-opercular (CO) network, also referred to as salience network (Fig.2A) (Dosenbach et al., 2006; Seeley et al., 2007). The anatomically selective mapping of α4β2 receptor density to this network generates a targeted hypothesis regarding the brain structures mediating the cognitive impact of the α4 polymorphism rs1044396.

The spatial relation between the CO network and α4β2 nAChR density suggests that functional differences in this receptor may impact the cognitive function of the CO network. Several lines of research suggest that one core cognitive control function of the CO network is the maintenance of sustained/tonic alertness, or vigilance (Sturm et al., 2004; Sadaghiani et al., 2010). Tonic alertness describes the mentally effortful, self-initiated (rather than externally driven) and continuous preparedness to process information and to respond (Parasuraman, 1998; Posner, 2008). A distinctive characteristic of the CO network is that it becomes active whenever cognitive engagement is required irrespective of the specific task (Dosenbach et al., 2006; Yeo et al., 2014), likely due to tonic alertness demands present across cognitive tasks (Sadaghiani and D'Esposito, 2015).

Here, we test the hypothesis that α4β2 nAChR genotype impacts CO network activation during cognitively demanding tasks, and explains performance differences in tonic alertness. We focus on the *CHRNA4* rs1044396 genotype in light of the above-described prior behavioral literature. We study the impact of this polymorphism on brain activity and behavior in a large dataset in adolescents, with replication in an independent cohort of adolescents and young adults.

Materials and Methods

Subjects

Adolescents and young adults of Caucasian descent were investigated in two cohorts, IMAGEN and Philadelphia Neurodevelopmental Cohort (PNC) as detailed in table 1. The IMAGEN cohort contains over 2000 subjects studied in eight cities across Europe. The cohort

and data acquisition are described in detail in (Schumann et al., 2010). All subjects were 14 years of age at time of data collection. We retained all subjects with SNP rs1044396 imputation accuracy >0.9 (See genetics below). Among these, n=1499 subjects had behavioral data in the Rapid Visual Processing task and n=1358 subjects had neuroimaging data in the Stop Signal Task (see fMRI section below). Pubertal development stage was determined for use as a covariate using the Puberty Development Scale (Petersen et al., 1988), a self-reported measure of physical development based on the scale introduced by Tanner (Tanner, 1978). On this five-category scale the vast majority of subjects had a puberty category score of 3 or 4 (median (IQR) = 4(1)).

From over 8000 American subjects studied in Philadelphia for the PNC cohort all those that identified as being of Caucasian descent (not including mixed ethnicities) were selected for ethnic homogeneity and comparability with the IMAGEN cohort (n=4734). The cohort and data acquisition are described in detail in (Satterthwaite et al., 2014, 2016). We retained all subjects with SNP rs1044396 imputation accuracy >0.9. For comparability with the IMAGEN dataset, only subjects of at least 14 years of age were included (age range 14-22). Among these, n=2151 had behavioral data in the Penn Continuous Performance Test experiment, and n=228 had neuroimaging data in the N-Back experiment.

------- *Table 1 here* -------

Genetics

IMAGEN subjects were genotyped from blood samples on 610-Quad SNP and 660-Quad SNP arrays from Illumina (Illumina Inc., San Diego, CA). The vast majority of PNC subjects were genotyped from blood samples on the 550HH and 610-Quad SNP arrays from Illumina (Illumina Inc., San Diego, CA). Since rs1044396 SNP was not included in the Illumina array platforms by IMAGEN and PNC consortia, we imputed *CHRNA4* rs1044396 using the Haplotype Reference Consortium r1.1. as reference panel (McCarthy, 2016). In the IMAGEN cohort, *CHRNA4* rs1044396 was successfully imputed for 89.3% of the subjects using the Sanger Imputation Service (https://imputation.sanger.ac.uk/) with EAGLE2 (Loh et al., 2016) and PBWT (Durbin, 2014); Minor Allele Frequency (MAF) was 0.479, as expected in Caucasians (European 1000 Genomes Consortium Phase3 (MAF=0.471) (The 1000 Genomes Project Consortium, 2015). In the PNC cohort, *CHRNA4* rs1044396 was successfully imputed for 88.4% of the subjects using the Michigan Imputation Server

(https://imputationserver.sph.umich.edu/) (Das et al., 2016) with SHAPEIT2 (Delaneau et al., 2013) and Minimac3 (Das et al., 2016). Note that while imputation was performed on different servers for the two cohorts because this process was completed at different instances and sites, both servers used an identical reference set. The MAF was 0.472. Genotype distribution did not deviate from Hardy-Weinberg Equilibrium in the IMAGEN (P=0.77) and PNC (P=0.99) cohorts.
LD analysis was performed using Haploview v.4.2, and defining LD blocks based on the solid spine of LD algorithm (Barrett et al., 2005). Haplotype-based association testing was performed using PLINK by logistic regression model, adjusting for the same covariates employed in the analysis of individual datasets. Results from each dataset were fixed-effect meta-analyzed using GWAMA (Mägi and Morris, 2010).

fMRI Acquisition

At IMAGEN sites, structural and functional MRI was performed on 3T scanners from a range of manufacturers (at Hamburg, Mannheim, Dresden, and Paris: Siemens Trio with 12-channel head coil, Siemens, Munich, Germany; at Berlin: Siemens Verio with 8- and 12-channel head coils; at Dublin and Nottingham: Philips Achieva with 8-channel head coil, Philips, Best, The Netherlands; at London: GE HDx with 8-channel head coil, General Electrics, Chalfont St Giles, UK). A set of imaging sequence parameters compatible with all scanners, particularly those directly affecting image contrast or signal-to-noise, was devised and held constant across sites. Functional imaging parameters consisted of 8 min echo planar imaging with TR/TE/Flip Angle = 2200ms / 30ms / 75°, 64x64x40 voxels with 2.4mm slice thickness and 1 mm slice gap and a field of view of 218x218mm, yielding isotopic 3.4mm voxels. The structural image consists of a T1weighted MPRAGE image of 256x256x160/166 voxels (depending on manufacturer), with a 1.1mm isotropic voxel size. Details are provided in (Schumann et al., 2010). Functional images in the PNC cohort were recorded on a Siemens TIM trio scanner with 32-channel head coil and consisted of 11.6 min echo planar imaging with TR/TE/Flip Angle = 3000ms / 32ms / 90°, 64x64x46 voxels with 3mm slice thickness and no slice gap and a field of view of 192x192mm, yielding isotopic 3mm voxels. The structural image consists of a T1-weighted MPRAGE image of 192x256x160 voxels, with a 0.9x0.9x1mm voxel size. Details are provided in (Satterthwaite et al., 2013, 2014).

Experimental Design

Tasks for fMRI: Both the IMAGEN and PNC datasets included neuroimaging during tasks demanding high cognitive engagement. In the IMAGEN dataset, among four fMRI runs (a

functional localizer and three other tasks) we chose to investigate the Stop-Signal Task due to its high cognitive control demands. This task requires subjects to press a left or a right button in response to regularly presented visual 'go' stimuli (left- or right-pointing arrows, respectively, every 1.6 to 2s) but to withhold response if the go stimulus was followed by a 'stop' signal (upwards-pointing arrow). The stop signal was presented unpredictably across trials and the time between the foregone go stimulus and the stop signal (stop signal delay) was adjusted continuously during the run so as to keep the individual subject's stop success at 50%. Stop signal delay (range 0-900ms) was increased or decreased from an initial duration of 150ms at the beginning of the experiment in steps of 50ms depending on the subject's stop success/failure (Rubia et al., 2005). There were 400 go trials and 87 stop trials.

In the PNC cohort, among the two available fMRI tasks, we chose to investigate the fractal N-Back task due to its demands on cognitive control (Satterthwaite et al., 2014). In this task subjects were presented with complex geometric figures (fractals) for 500ms at a fixed 2500ms interstimulus interval. In different block conditions, subjects pressed a button if they detected a predefined target fractal (0-back condition), if the current fractal was identical to the previous one (1-back condition), or if the current fractal was identical to the fractal two trials previously (2-back condition). Visual instructions (9 s) preceded each block, informing the participant of the upcoming condition. Each condition was performed in three blocks of 20 trials (60s) each. There were a total of 45 targets and 135 foils with 1:3 ratio in each block. A 24s passive fixation period was presented at the beginning, middle and end of the task.

Tasks for behavioral assessments: CPTs are available as part of larger cognitive test batteries in both cohorts. The Cambridge Neuropsychological Test Automated Battery (CANTAB http://www.cambridgecognition.com) acquired in the IMAGEN cohort includes the Rapid Visual Processing CPT task. This task requires subjects to detect a predefined target series of 3 digits in a continuous stream of digits (2 through 9) presented at a rate of 100/min. There were 27 occurrences of the target sequence during the 8 min experimental run. Accuracy in this task is commonly measured using *A'* (Gau and Huang, 2014). *A*' is defined as $0.5+[(h-f)+(h-f)^2]/[4\times h\times(1-f)]$, where h is the probability of hits and f is the probability of false alarms. *A'* is a signal detection measure of sensitivity to the target, regardless of response tendency. It takes into account both hits and false alarms and is directly comparable to the classical index of sensitivity *d'* (see below) (Sahgal, 1987). However, it is based on a non-parametric signal detection model suitable for the Rapid Visual Processing task where the

sensory effects of stimulus-triplets may not be well-represented by the normal distribution. Difference in *A'* across genotypes was tested using multiple regression.

The Penn Computerized Neurocognitive Battery (Penn CNB) acquired in the PNC cohort includes the Penn Continuous Performance Test (Kurtz et al., 2001). This task presents a stream of 7-segment displays (connected horizontal and vertical lines) at a rate of 60/min. The subjects were required to press a button whenever the display formed a digit (first half of experiment) or a letter (second half of experiment). There were 60 occurrences of targets (30 digits and 30 letters) during a total of 6 min. Accuracy was measured as sensitivity to the target regardless of response tendency, using the classical sensitivity index $d' = Z(h) - Z(f)$, where $Z(p)$ is the inverse of the cumulative distribution function of the Gaussian distribution. Hit rates (h) of 1 were replaced with (n - 0.5)/n, and false alarm rates (f) of 0 were replaced with 0.5/n, where n is the number of targets or non-targets, respectively (Macmillan and Kaplan, 1985). Difference in *d'* across genotypes was tested using multiple regression.

Statistical Analysis

fMRI preprocessing: The fMRI data provided on the IMAGEN database were already slice timing corrected, motion corrected, and spatially normalized to MNI space using SPM8 (http://www.fil.ion.ucl.ac.uk/spm/). For PNC fMRI data we applied motion correction and spatial normalization to MNI space using ANTs (http://stnava.github.io/ANTs/). Further preprocessing was equivalent across IMAGEN and PNC datasets, which included regressing out six linear head motion parameters, white matter and cerebrospinal fluid confounds (based on segmentation, thresholded at 95% tissue type probability), five principal components of high variance voxels derived using CompCor (Behzadi et al., 2007), and one-time sample shifted variants as well as discrete cosine functions (for high-pass filtering at 1/128 Hz) of all confound regressors. Our volumes of interest were large-scale networks defined using independent component analysis of resting-state functional connectivity in an independent dataset as available in the 90-region FIND lab atlas (Shirer et al., 2012). Large-scale functional networks defined on the basis of their intrinsic connectivity architecture during resting state provide volume delineation unbiased by particular task-related activation. To this end, the use of an independent atlas permits application of the same volume of interest to both cohorts. Note that no resting state data was available for a subject-specific definition of networks for the majority of IMAGEN subjects. Time courses were extracted from all voxels across the brain areas of each network, averaged to yield one time course per network and normalized to z-scores.

In addition to accounting for head motion with the above-described motion parameters, their time shifted variants and discrete cosine functions, we verified that head motion did not substantially contribute to between-group effects using mean framewise displacement (MFD) as a measure (Power et al., 2012). Relatively few volumes per subject showed displacement > 3 standard deviations above the average MFD across all subjects (IMAGEN 16.1 (=3.6%) ±30.7 volumes, and PNC 10.9 (4.7%) ±15.5 volumes per subject). Further, only few subjects had an MFD > 3 standard deviations over the group average MFD (25 (1.8%) IMAGEN subjects, and 5 (2.2%) PNC subjects). Therefore, we did not exclude any subjects or fMRI volumes based on head motion. Direct contrast of MFD across genotypes ensured that head motion did not differ significantly between T/T, T/C and C/C carriers ($p>0.4$ for all pair-wise *t*-tests in IMAGEN and PNC).

fMRI General Linear Models: Analyses were performed using in-house MATLAB code. In IMAGEN's Stop Signal Task, successful go trials densely covered the experimental run and thus served as implicit baseline. The time course of all other events, i.e. successfully inhibited stop trials, inhibition failures on stop trials, left-right errors on go trials and errors of omission (not responded in time on go trials) were convolved with the canonical hemodynamic response function to yield regressors of interest. A General Linear Model was constructed with these regressors for each subject and each network's time-course averaged across all the respective voxels (CO, fronto-parietal, dorsal attention and default mode networks) as response. An equivalent GLM analysis was performed for the whole brain using voxel-wise time-courses as response. The contrast of interest comprised the sum of the respective regression coefficient estimates. Errors of omission were absent in 20% of participants, very sparse in the other subjects and therefore excluded from the contrast. At the group level, the resulting contrast value entered multiple regression with genotypes as regressor of interest.

The whole-brain voxelwise statistics in the IMAGEN cohort was derived by restricting the overdominance contrast volume (T/C carriers > other subjects) to the union of all 116 AAL atlas regions as lenient generic grey matter mask, and applying an auxiliary uncorrected threshold of $p<0.005$ (two-sided *t*-test) followed by cluster-level correction for multiple comparisons. Covariates of no interest were co-regressed. The cluster size for this correction was determined using a Monte Carlo simulation with 1000 permutations of randomized genotypes using in-house MATLAB code.

In PNC's N-back Task, regressors were generated by convolving the canonical hemodynamic response function with the boxcar time course of 0-back, 1-back and 2-back blocks. Additionally, we modeled pre-block instructions (9s) as an additional regressor of no interest to account for the respective brain processes. A General Linear Model was constructed with these regressors for each subject, and the time-course averaged across all the voxels of the network volume-of-interest as response. The contrast of interest comprised the sum of the regression coefficient estimates of 0-back, 1-back and 2-back blocks. At the group level, the resulting contrast value was entered into multiple regression as response, with genotypes as regressor of interest.

For data quality assurance, subjects for which the estimated BOLD response in any of the network volumes-of-interest deviated by > 3 SD from the mean were excluded from fMRI group statistics (33 subjects in IMAGEN, none in PNC).

Group-level regression (fMRI and behavioral): An initial model compared fMRI signal across rs1044396 genotypes with no a priori assumption on the genetic model of association, using two binary regressors to encode genotypes, with the values 0 0 for T/T, 1 0 for T/C, and 0 1 for C/C. In subsequent models that specifically tested for presence of overdominance, a binary regressor with 1 encoding T/C carriers and 0 encoding T/T and C/C carriers was used, hence testing T/C heterozygotes against T/T and C/C homozygotes. For the IMAGEN cohort, covariates of no interest comprised sex, puberty score, scan site (7 categorical covariates) and population structure (first 3 principal components). For the PNC cohort, covariates of no interest included sex, age and population structure (first 3 principal components).

Results

CO network activation was investigated using fMRI of tasks that have high cognitive demands known to engage this network (Whelan et al., 2012; Satterthwaite et al., 2013). Behavior was studied using Continuous Performance Tests (CPTs) whose continuous nature is specifically designed and widely used to selectively measure tonic alertness or vigilance (Beck et al., 1956; Kurtz et al., 2001).

CHRNA4 polymorphism and cingulo-opercular network activation

We hypothesized that activity in the CO network during cognitive engagement is affected by rs1044396 genotype. The CO network volume of interest was taken from a functional atlas

derived from resting-state functional connectivity analysis of an independent sample (Fig 1A. (Shirer et al., 2012)). In the IMAGEN fMRI dataset (n=1358, see table 1), we investigated network activity during a Stop-Signal Task that requires a high level of cognitive control. Subjects had to press a button in response to regularly presented go stimuli but withhold response if the go stimulus was followed by a stop signal. Note that although this task requires several other cognitive control functions such as top-down inhibition and spatial attention, it is known to heavily involve tonic alertness and the CO network (Satterthwaite et al., 2013). For each subject, the CO network fMRI signal time course was entered in a General Linear Model (GLM) comprising regressors for all estimable task events. Estimated brain activity across these events confirmed strong engagement of the CO network volume of interest across all subjects irrespective of genotype (one sample *t*-test t_{1357}=54.57, $p<10^{-10}$). With T/T (homozygous carriers of the major allele) as the baseline, we examined the effects of the presence of minor allele C, i.e. T/C and C/C genotypes, on CO network activity using multiple regression with no a priori assumption on the genetic model of association. Task-related activity in this network was significantly higher in T/C carriers compared to T/T carriers (t_{1343}=2.83, p=0.005; Figure 1), while activity for C/C carriers did not differ from T/T carriers (t_{1343}=-0.003, p=0.998). This result is suggestive of an overdominant effect, where the phenotype of heterozygotes lies outside the phenotypical range of both homozygous groups due to allelic interaction at a single locus (Hochholdinger and Hoecker, 2007). Following this observation, we used multiple regression to specifically test for overdominance, i.e. T/C carriers > all other subjects. This analysis confirmed higher CO network activity in heterozygotes as compared to homozygotes (t_{1344}=3.44, p=0.0006, 0.9% variance explained).

------ Figure 1-------

Figure 1: Heterozygotes at the CHRNA4 SNP have increased cingulo-opercular network activation. A) The CO network volume of interest in the FINDlab atlas based on intrinsic functional connectivity (Shirer et al., 2012). B) Estimated brain activation averaged across the CO network volume of interest in the IMAGEN cohort during the Stop Signal Task. Higher CO network activation is observed in heterozygotes compared to homozygous T/T and C/C carriers. On boxes, the central mark indicates the median, and the bottom and top edges indicate 25th and 75th percentiles, respectively. The whiskers extend to the most extreme data points not considered outliers (within 1.5 interquartile range of the bottom and top of box), and the outliers are marked by '+'. C) The genotype contrast T/C > homozygotes is shown for activation in the CO network and three other networks for comparison: FP = fronto-parietal, DAT = dorsal

attention, DM = default mode. A significant overdominant effect was observed for the CO network only. Error bars show standard error.

To test the neuroanatomical specificity of rs1044396 impact on the CO network, we investigated three other high-level networks as controls. These comprised the default mode network as well as two networks underlying other cognitive control functions, namely the dorsal attention network supporting selective attention, and the lateral fronto-parietal network supporting phasic adaptive control. Using identical first and second level GLM analyses, neither T/C nor C/C carriers showed significant differences in network activation compared to T/T carriers in these three control networks (all $t_{1343}<1.2$), nor was an effect observed when comparing T/C against both homozygous groups (all $t_{1344}<1.6$, Figure 1C).

To further investigate this neuroanatomical specificity, we complemented our volume of interest-based approach with whole-brain voxel-wise regression. Contrasting T/C carriers with homozygotes, we found significantly higher activity in T/C carriers across several cortical areas of the CO network (cluster-level corrected based on Monte Carlo permutation test, following an auxiliary uncorrected threshold $p<0.005$). These nodes comprised right and left anterior insulae, right and left anterior prefrontal cortices, and left dorsal anterior cingulate cortex (Fig 2, table 2). The clusters showed anatomical overlap and correspondence with all five cortical areas of the CO network as defined by the FIND atlas (Shirer et al., 2012). We found additional significant clusters largely located in sensory and motor processing regions (table 2) that may represent task-specific processing top-down modulated by higher cognitive control engagement of the CO network in heterozygotes.

------ Figure 2-------

Figure 2: The whole-brain map shows that activation differences across genotypes overlap with the CO network. Shown is the contrast T/C larger than homozygous T/T and C/C carriers in the IMAGEN cohort during the Stop Signal Task ($p<0.005$ auxiliary uncorrected threshold, corrected at cluster-level). Blue shows the CO volume of interest as in Fig. 1, red shows areas of higher activation in heterozygotes, displayed on a canonical single subject structural image, demonstrating the overlap in dorsal anterior cingulate, anterior prefrontal and anterior insula loci.

--------- *Table 2 here* ---------

We tested whether an overdominant effect could be confirmed in the independent PNC fMRI dataset (n=228). This cohort completed an n-back task that requires subjects to monitor a continuous stream of abstract geometric images for specific stimulus repeats. In different block conditions, subjects pressed a button if they detected a predefined target image (0-back condition), if the current image was identical to the previous one (1-back condition), or if the current image was identical to the image two trials previously (2-back condition). Again, we investigated brain activity evoked by all estimable events (0-back, 1-back and 2-back trials). Strong engagement of the CO network was confirmed across all subjects irrespective of genotype (one sample *t*-test t_{227}=12.50, $p<10^{-10}$). Activation in the CO network was then compared across subjects with rs1044396 T/T, T/C and C/C genotypes (Figure 3A). Using multiple regression we tested for overdominance, i.e., T/C carriers > all other subjects. This analysis confirmed higher CO network activation in heterozygotes as compared to homozygotes (t_{221}=2.77, p=0.006, 3.4% variance explained).

Note that beyond increased demands on tonic alertness, the n-back task requires considerable working memory engagement. This task is thus commonly used to extract working memory processes associated with regions of the fronto-parietal network, especially the dorsolateral prefrontal cortex (Owen et al., 2005; D'Esposito and Postle, 2015). Indeed, while the fronto-parietal network was activated by this task (one sample *t*-test irrespective of genotype t_{227}=4.31, $p<10^{-4}$), no significant activation difference was found across genotypes in this network or the other two networks, dorsal attention and default mode networks, that we investigated as controls (all t_{221}<0.8 for T/C against homozygotes, Figure 3B). This result again speaks to the anatomical specificity of the impact of rs1044396 on CO network activation.

------ Figure 3 -------

Figure 3: Increased cingulo-opercular network activation in heterozygotes is replicated in the PNC cohort. A) Estimated brain activation averaged across the CO network volume of interest in the PNC cohort during the fractal N-back task is shown separately for each genotype. Higher CO network activation is observed in heterozygotes compared to homozygous T/T and C/C carriers. Boxplots are arranged as explained in Figure 1. B) The genotype contrast T/C > homozygotes is shown for activation in the CO network and three other networks for comparison (abbreviations as in Fig. 1). A significant overdominant effect was observed for the CO network only. Error bars show standard error.

CHRNA4 rs1044396 and tonic alertness

After observing that the rs1044396 polymorphism is associated with the strength of activation in brain areas maintaining tonic alertness, we next asked whether this impact translates into inter-individual differences in behavioral measures of tonic alertness. Tonic alertness, the intrinsically maintained preparedness to process information and to respond, is a necessary prerequisite for more specialized cognitive functions such as selective attention and perceptual processes to build on. In contrast to selective attention and phasic stimulus-driven alertness, tonic alertness is continuous rather than transient (Posner and Boies, 1971), and has a general overarching nature, rather than operating with respect to specific information and sensory features (Robertson and Garavan, 2004).

Note that the tasks for which fMRI data were available co-engaged multiple higher order cognitive processes, rendering the selective investigation of alertness difficult. Hence, to study behavior we turned instead to behavioral CPTs that selectively target tonic alertness. The IMAGEN study contains a visual CPT called Rapid Visual Processing, during which subjects (n=1499) continuously attend a visual stream of digits and press a button whenever a predefined target sequence of 3 digits is detected. Performance accuracy (*A'*) was compared across rs1044396 genotypes. Paralleling the neuroimaging findings, we tested for presence of overdominance (i.e. T/C carriers > all other subjects) and found that heterozygotes showed the highest performance accuracy (t_{1485}=2.28, p=0.023, 0.4% variance explained). For completeness, we also comprehensively investigated behavior during the fMRI SST task (individual Stop-Signal Delay, Stop-Signal reaction time, reaction time on Go trials, failures to stop, and left-right errors). We found no significant impact of genotype, presumably because of dependence of performance in this task on multiple overlapping cognitive control faculties, in line with lack of behavioral effects during the two previous neuroimaging studies of rs1044396 (Winterer et al., 2007; Gießing et al., 2012).

We then attempted to replicate the presence of overdominance at rs1044396 on behavior in the independent PNC cohort. PNC uses a visual CPT during which subjects (n=2151) continuously attend a visual stream of figures made of seven lines and press a button whenever the lines form a digit or a letter. Performance accuracy (*d'*) was compared across subjects with rs1044396 T/T, T/C and C/C genotypes (Figure 4B). This analysis confirmed higher performance accuracy in heterozygotes as compared to T/T and C/C carriers (t_{2144}=3.18, p=0.0015, 0.5% variance explained).

------ Figure 4 -------

Figure 4: The impact of genotype on tonic alertness capacity shows an overdominant effect. Performance accuracy in Continuous Performance Tests (CPTs) as measured by perceptual sensitivity is shown for the IMAGEN (A) and PNC (B) cohorts for the three rs1044396 genotypes. In both datasets, heterozygotes performed better than homozygote carriers of the major ("T") or minor ("C") allele. Boxplots are arranged as explained in Figure 1.

Meta-analysis of overdominance

Finally, to investigate the cumulative evidence gained from IMAGEN and PNC cohorts for overdominance at rs1044396 (T/C > [T/T C/C]) in fMRI and behavioral data, we performed a meta-analysis over the respective effect sizes. We found z=4.36, $p=1.33*10^{-5}$ (total n=1586) for the fMRI measures of CO activation, and z=2.54, p=0.011 (total n=3650) for behavioral measures of alertness. The behavioral meta-analysis under-performed compared to the fMRI meta-analysis presumably due to heterogeneity of the behavioral measure across the two cohorts (behavioral: q=8.88, p = 0.003; fMRI: q=0.5, p=0.48).

CHRNA4 overdominance and haplotypes

To further elucidate whether the observed overdominant effect was due to allelic interaction at the SNP of interest, or resulting from heterozygosity at multiple neighboring locations (pseudo-overdominance, see Discussion section), we performed haplotype association tests for the linkage disequilibrium (LD) block surrounding rs1044396, which includes 28 SNPs. Eleven haplotypes with frequency above 1% were considered for the analysis. Haplotype frequencies are comparable between IMAGEN and PNC, with H1 haplotype, which includes the rs1044396-T allele, being the most frequent (38%) in both IMAGEN and PNC cohorts. We found no significant association of CO network activation levels or behavioral measures of alertness for haplotypes of the surrounding *CHRNA4* region in either cohort (the omnibus tests were not significant, and no individual haplotype showed a significant association). This result speaks against pseudo-overdominance in favor of a true overdominant effect at rs1044396.

CHRNA4 rs1044396 and gene expression levels

The potential biological mechanisms underlying the observed impact of the synonymous SNP rs1044396 remains unclear. While the SNP has no effect on the amino acid level, the change from T to C disrupts a potential methylation site (CpG). Indeed, the entire exon 5 of CHRNA4 overlaps with a CpG island (UCSC genome browser (Kent et al., 2002)). Thus, we investigated the dependence of *CHRNA4* expression in neural tissue on this polymorphism using publicly

available data from the Genotype-Tissue Expression (GTEx) project (The GTEx Consortium, 2015). Based on the focus of our neuroimaging investigations on large-scale cortical networks, we investigated the two available cortical regions Brodmann Area 9 (samples=92; in the vicinity to BA46 that encompasses the anterior prefrontal region of CO network; cf. Fig. 1A), and Brodmann Area 24 (samples=72; directly overlapping with the anterior cingulate cortex region of the CO network). Additionally, we analyzed the Tibial Nerve, because much higher tissue samples were available for it compared to brain tissues (samples=256). In all investigated neural tissue, we found a linear dosage effect, such that homozygous major allele carriers (T/T) had the highest expression levels, and heterozygotes showed intermediate gene expression (Brodmann Area 9 t=4.3, p=6*10^{-5}, Brodmann Area 24 t=2.6, p=0.011; Tibial Nerve t=5.4, p=2*10^{-7}). This analysis shows that rs1044396 is an expression quantitative trait locus (eQTL) modulating expression levels of *CHRNA4*.

Discussion

While the nicotinic system plays an important role in cognitive control processes, the contribution of genetic variability in this system to (nicotine consumption-unrelated) cognition has received scant attention (Greenwood et al., 2012). Furthermore, it is not well understood whether any specific brain structures are affected by the genetic makeup of the nicotinic system. Here, we investigated the relation between brain activity and behavior with a common SNP of the most prevalent, high affinity nicotinic receptor in the brain. Specifically, based on our prior findings of nicotinic receptor distribution (Picard et al., 2013), we expected the rs1044396 genotype to impact neural activity in the CO network. Additionally, based on the previously established link between the CO network and sustained alertness (Sadaghiani and D'Esposito, 2015), we expected an impact of this polymorphism on the ability to engage this cognitive control function. The CO network is known to show pervasive activation across numerous distinct cognitive tasks. This general activation profile allowed us to study the CO network in previously acquired fMRI experiments across two large cohorts. We found that during cognitive engagement the CO network, but not other control-related networks, showed higher activity in heterozygotes (T/C carriers) as compared to homozygous carriers of the major (T/T) or minor allele (C/C). Furthermore, we observed that heterozygotes performed at significantly higher accuracy in behavioral tasks that primarily depend on the ability to maintain alertness. Findings were consistent across both cohorts totaling N=1586 subjects for neuroimaging and N=3650 for behavior. These results therefore expand considerably upon encouraging, but relatively underpowered (N<50), neuroimaging studies of this SNP (Winterer et al., 2007; Gießing et al., 2013). One of these studies found highest task-related activity in T/T homozygotes in

supplementary motor/anterior cingulate cortex and left postcentral gyrus (Winterer et al., 2007). Conversely, the other study, which did not include heterozygous subjects, found higher activity for C/C compared to T/T carriers in right middle temporal, but lower activity in right superior temporal gyrus (Gießing et al., 2012). Our results constitute the first report of overdominance in a *CHRNA4* association study of brain activity and cognitive performance. This overdominant effect may be one contributor to discrepancy in impact from T vs. C alleles in previous behavioral and fMRI studies with smaller sample sizes.

Possible mechanisms underlying overdominance

What could be driving the observed overdominant effect? Overdominance is often missed because the most prevalent genetic models used in Genome-wide Association Studies (GWAS) rely on the a-priori assumption that alleles contribute to complex traits in a linear additive fashion. However, overdominance is expected to be very prevalent (Comings and MacMurray, 2000). One common source of overdominance is thought to be the interaction among multimeric protein products (Comings and MacMurray, 2000). The α4β2 nicotinic receptor is a pentamer and commonly contains two α4 subunits, readily suggesting functional interactions between these subunits. However, rs1044396 leads to a synonymous amino-acid substitution and it seems unlikely that such modification would affect α4 multimerization. A more plausible explanation could relate to a pseudo-overdominant effect (Draghi and Whitlock, 2015) due to the presence of multiple, cis-acting *CHRNA4* SNPs in the LD block including rs1044396, which may favor the expression of a particular haplotype over-represented in rs1044396 heterozygotes. However, according to our haplotype analysis we can exclude the existence of cis-interacting SNPs at the rs1044396-LD block. At the same time, we should not ignore the possibility of a hidden interaction between rs1044396 and another genetic/environmental factor (e.g., SNPxSNP interaction, SNPxEnvironment interaction). The possibility of a SNPxEnvironment interaction is supported by the fact that rs1044396 is followed by a “G” nucleotide, thus creating a potential methylation site (CpG) in rs1044396 C-allele carriers, which is absent in rs1044396 T-allele carriers.

Overdominance and functional advantage of intermediate expression levels

A source for overdominance at rs1044396 could be an advantage of intermediate *CHRNA4* expression levels, possibly modulated by the methylation site. One of the best-known examples of overdominance is the non-synonymous (Val→Met) SNP rs4680 of the *COMT* gene. *COMT* encodes the dopamine-metabolizing enzyme catechol-O-methyltransferase, with

650 the Met variant (T-allele) showing a dosage effect on prefrontal dopamine concentrations.
651 Association of cognitive performance with prefrontal dopamine often follows an inverted U-
652 shape. Thus, intermediate dopamine levels observed in heterozygous carriers result in better
653 performance in specific cognitive tasks compared to homozygous C/C and T/T carriers (Cools
654 and D'Esposito, 2011). An analogous effect could underlie our overdominance observations of
655 *CHRNA4*, such that having one rs1044396 T-allele would result in intermediate expression
656 levels of the corresponding α4 protein. This interpretation is strongly supported by our finding
657 that rs1044396 is an eQTL for *CHRNA4*, resulting in intermediate gene expression levels in
658 heterozygotes. Since *CHRNA4* likely affects receptor sensitivity to acetylcholine (Eggert et al.,
659 2015), intermediate expression levels might be optimal for certain functions such as those
660 underlying maintenance of tonic alertness, resulting in heterosis (superior phenotype of
661 heterozygotes).
662
663 The optimal expression level however, might be dependent on the cognitive function
664 under investigation. In the context of *COMT,* the ideal prefrontal dopamine level (i.e., the peak
665 of the inverted U-shape function) is task-dependent, resulting in discrepancies across *COMT*
666 association studies (Cools and D'Esposito, 2011). An inverted U-function could drive a similar
667 task-dependence for rs1044396 effects and explain the contradictory reports in behavioral
668 association studies (Störmer et al., 2012). While the high density of α4β2 receptors in the CO
669 network suggests an especially prominent role of *CHRNA4* polymorphisms in sustained
670 alertness, other cognitive control functions are likely affected as well. The association of
671 rs1044396 genotype with performance might differ for tasks that primarily rely on sustained
672 alertness (such as CPT tasks studied here) compared to those targeting phasic and selective
673 control functions such as spatial attention or cued orienting investigated in previous studies
674 (Greenwood et al., 2005, 2005; Espeseth et al., 2010). Such task-dependence may also explain
675 the different findings in the two previous brain imaging studies of rs1044396 that focused on
676 selective attention tasks (Winterer et al., 2007; Gießing et al., 2012).
677
678 *Limitations*
679 One limitation to making use of previously acquired datasets is that we were not able to
680 administer an ideal task specific to tonic alertness. Rather, we had to interrogate tonic alertness
681 as a cognitive control function that was common to the cognitively demanding tasks examined
682 here. The available neuroimaging tasks heavily involved more specific functions such as
683 response inhibition (Stop-Signal task in IMAGEN) and working memory (N-back task in PNC) in

addition. This co-engagement of cognitive functions limits an unequivocal interpretation of the neuroimaging effects as tonic alertness. However, the fact that two very different tasks resulted in comparable overdominant effects supports the interpretation that rs1044396 impacts an omnipresent cognitive control function shared across the respective tasks. The observation of overdominant effects in behavioral CPT procedures that selectively target tonic alertness suggests that this general control function might constitute alertness.

Another potential limitation of our study, and a difference from previous association studies of rs1044396, is the subjects' age. The IMAGEN and PNC cohorts consist of adolescents and young adults, while the average age in previous behavioral studies has commonly spanned mid-30s and higher (Greenwood et al., 2005; Parasuraman et al., 2005; Reinvang et al., 2009). It is conceivable that the genotype effects observed in our cohorts change across the lifespan beyond the age range that we investigated. This question should be addressed in future studies using neuroimaging and genetics cohorts at other ages. A potential difference in *CHRNA4* genotype effect between teen-aged subjects and older subjects would provide an important step forward in understanding genetic contributions to individual brain development during puberty.

Finally, the hypothesis-driven investigation of a single common SNP may present a potential limitation in terms of overall functional impact. Common SNPs generally have small effect sizes, and are only a small piece of a large picture in the explanation of complex traits and their neural substrate.

Conclusions

In this association study of the high-affinity nicotinic receptor α4β2 in two large cohorts, we establish the importance of the CO network in mediating neuromodulatory effects of acetylcholine on cognition. We further provide a piece of the genetic puzzle underlying inter-individual differences in the foundational ability to maintain alertness. These insights into the role of genetic variability in brain activation and cognitive control may help understand how genetic changes translate into aberrant behavior in various disorders of cognitive control. This line of work may facilitate individualized medicine in the future by informing how particular neuropharmacological treatments will affect individual patients' brain activity and cognition based on their genotype. The specific study of nicotinic receptors can further lend insights into the basis of individuals' susceptibility to nicotine addiction as it depends on brain activity and

718 cognitive control profile. In summary, the current findings establish a connection between
719 *CHRNA4* genotype, CO network activation and sustained alertness, providing insights into
720 brain-behavior relations and how genetics shapes this relation.
721
722 **References**
723 Albuquerque EX, Pereira EFR, Alkondon M, Rogers SW (2009) Mammalian Nicotinic
724 Acetylcholine Receptors: From Structure to Function. Physiol Rev 89:73–120.

725 Barrett JC, Fry B, Maller J, Daly MJ (2005) Haploview: analysis and visualization of LD and
726 haplotype maps. Bioinformatics 21:263–265.

727 Beck LH, Bransome ED Jr, Mirsky AF, Rosvold HE, Sarason I (1956) A continuous
728 performance test of brain damage. J Consult Psychol 20:343–350.

729 Behzadi Y, Restom K, Liau J, Liu TT (2007) A component based noise correction method
730 (CompCor) for BOLD and perfusion based fMRI. NeuroImage 37:90–101.

731 Breitling LP, Dahmen N, Mittelstraß K, Rujescu D, Gallinat J, Fehr C, Giegling I, Lamina C,
732 Illig T, Müller H, Raum E, Rothenbacher D, Wichmann H-E, Brenner H, Winterer G
733 (2009) Association of nicotinic acetylcholine receptor subunit α4 polymorphisms with
734 nicotine dependence in 5500 Germans. Pharmacogenomics J 9:219–224.

735 Chang Z, Lichtenstein P, Asherson P, Larsson H (2013) Developmental twin study of attention
736 problems: High heritabilities throughout development. JAMA Psychiatry 70:311–318.

737 Comings DE, MacMurray JP (2000) Molecular Heterosis: A Review. Mol Genet Metab 71:19–
738 31.

739 Cools R, D'Esposito M (2011) Inverted-U–Shaped Dopamine Actions on Human Working
740 Memory and Cognitive Control. Biol Psychiatry 69:e113–e125.

741 Das S et al. (2016) Next-generation genotype imputation service and methods. Nat Genet
742 48:1284–1287.

743 Delaneau O, Zagury J-F, Marchini J (2013) Improved whole-chromosome phasing for disease
744 and population genetic studies. Nat Methods 10:5–6.

745 D'Esposito M, Postle BR (2015) The Cognitive Neuroscience of Working Memory. Annu Rev
746 Psychol 66:115–142.

747 Dosenbach NUF, Visscher KM, Palmer ED, Miezin FM, Wenger KK, Kang HC, Burgund ED,
748 Grimes AL, Schlaggar BL, Petersen SE (2006) A core system for the implementation of
749 task sets. Neuron 50:799–812.

750 Draghi J, Whitlock MC (2015) Overdominance interacts with linkage to determine the rate of
751 adaptation to a new optimum. J Evol Biol 28:95–104.

752 Durbin R (2014) Efficient haplotype matching and storage using the positional Burrows–
753 Wheeler transform (PBWT). Bioinformatics 30:1266–1272.

754 Eggert M, Winterer G, Wanischeck M, Hoda J-C, Bertrand D, Steinlein O (2015) The nicotinic
755 acetylcholine receptor alpha 4 subunit contains a functionally relevant SNP Haplotype.
756 BMC Genet 16:46.

757 Espeseth T, Sneve MH, Rootwelt H, Laeng B (2010) Nicotinic Receptor Gene CHRNA4
758 Interacts with Processing Load in Attention. PLoS ONE 5:e14407.

759 Feng Y, Niu T, Xing H, Xu X, Chen C, Peng S, Wang L, Laird N, Xu X (2004) A Common
760 Haplotype of the Nicotine Acetylcholine Receptor α4 Subunit Gene Is Associated with
761 Vulnerability to Nicotine Addiction in Men. Am J Hum Genet 75:112–121.

762 Friedman NP, Miyake A, Young SE, DeFries JC, Corley RP, Hewitt JK (2008) Individual
763 differences in executive functions are almost entirely genetic in origin. J Exp Psychol
764 Gen 137:201–225.

765 Gallezot J-D, Bottlaender M, Grégoire M-C, Roumenov D, Deverre J-R, Coulon C, Ottaviani M,
766 Dollé F, Syrota A, Valette H (2005) In Vivo Imaging of Human Cerebral Nicotinic
767 Acetylcholine Receptors with 2-18F-Fluoro-A-85380 and PET. J Nucl Med 46:240–247.

768 Gau SS-F, Huang W-L (2014) Rapid visual information processing as a cognitive
769 endophenotype of attention deficit hyperactivity disorder. Psychol Med 44:435–446.

770 Gießing C, Neber T, Thiel CM (2012) Genetic variation in nicotinic receptors affects brain
771 networks involved in reorienting attention. NeuroImage 59:831–839.

772 Gießing C, Thiel CM, Alexander-Bloch AF, Patel AX, Bullmore ET (2013) Human Brain
773 Functional Network Changes Associated with Enhanced and Impaired Attentional Task
774 Performance. J Neurosci 33:5903–5914.

775 Greenwood PM, Fossella JA, Parasuraman R (2005) Specificity of the Effect of a Nicotinic
776 Receptor Polymorphism on Individual Differences in Visuospatial Attention. J Cogn
777 Neurosci 17:1611–1620.

778 Greenwood PM, Parasuraman R, Espeseth T (2012) A cognitive phenotype for a polymorphism
779 in the nicotinic receptor gene CHRNA4. Neurosci Biobehav Rev 36:1331–1341.

780 Gruszka A, Matthews G, Szymura B (2010) Handbook of Individual Differences in Cognition:
781 Attention, Memory, and Executive Control. Springer Science & Business Media.

782 Hendrickson LM, Guildford MJ, Tapper AR (2013) Neuronal nicotinic acetylcholine receptors:
783 common molecular substrates of nicotine and alcohol dependence. Addict Disord Behav
784 Dyscontrol 4:29.

785 Higley MJ, Picciotto MR (2014) Neuromodulation by Acetylcholine: Examples from
786 Schizophrenia and Depression. Curr Opin Neurobiol 0:88–95.

787 Hochholdinger F, Hoecker N (2007) Towards the molecular basis of heterosis. Trends Plant Sci
788 12:427–432.

789 Kent WJ, Sugnet CW, Furey TS, Roskin KM, Pringle TH, Zahler AM, Haussler and D (2002)
790 The Human Genome Browser at UCSC. Genome Res 12:996–1006.

791 Knott V, Bosman M, Mahoney C, Ilivitsky V, Quirt K (1999) Transdermal Nicotine: Single
792 Dose Effects on Mood, EEG, Performance, and Event-Related Potentials. Pharmacol
793 Biochem Behav 63:253–261.

794 Kozak R, Bruno JP, Sarter M (2006) Augmented Prefrontal Acetylcholine Release during
795 Challenged Attentional Performance. Cereb Cortex 16:9–17.

796 Kurtz MM, Ragland JD, Bilker W, Gur RC, Gur RE (2001) Comparison of the continuous
797 performance test with and without working memory demands in healthy controls and
798 patients with schizophrenia. Schizophr Res 48:307–316.

799 Lesh TA, Niendam TA, Minzenberg MJ, Carter CS (2011) Cognitive Control Deficits in
800 Schizophrenia: Mechanisms and Meaning. Neuropsychopharmacology 36:316–338.

801 Loh P-R, Danecek P, Palamara PF, Fuchsberger C, Reshef YA, Finucane HK, Schoenherr S,
802 Forer L, McCarthy S, Abecasis GR, Durbin R, Price AL (2016) Reference-based phasing
803 using the Haplotype Reference Consortium panel. Nat Genet 48:1443–1448.

804 Macmillan NA, Kaplan HL (1985) Detection theory analysis of group data: estimating sensitivity
805 from average hit and false-alarm rates. Psychol Bull 98:185–199.

806 Mägi R, Morris AP (2010) GWAMA: software for genome-wide association meta-analysis.
807 BMC Bioinformatics 11:288.

808 McCarthy S (2016) A reference panel of 64,976 haplotypes for genotype imputation. Nat Genet
809 48:1279–1283.

810 Mennes M, Zuo X-N, Kelly C, Di Martino A, Zang Y-F, Biswal B, Castellanos FX, Milham MP
811 (2011) Linking inter-individual differences in neural activation and behavior to intrinsic
812 brain dynamics. NeuroImage 54:2950–2959.

813 Owen AM, McMillan KM, Laird AR, Bullmore E (2005) N-back working memory paradigm: A
814 meta-analysis of normative functional neuroimaging studies. Hum Brain Mapp 25:46–59.

815 Parasuraman R (1998) The attentive brain. Cambridge, MA: MIT Press.

816 Parasuraman R, Greenwood PM, Kumar R, Fossella J (2005) Beyond Heritability
817 Neurotransmitter Genes Differentially Modulate Visuospatial Attention and Working
818 Memory. Psychol Sci 16:200–207.

819 Petersen AC, Crockett L, Richards M, Boxer A (1988) A self-report measure of pubertal status:
820 Reliability, validity, and initial norms. J Youth Adolesc 17:117–133.

Picard F, Sadaghiani S, Leroy C, Courvoisier DS, Maroy R, Bottlaender M (2013) High density of nicotinic receptors in the cingulo-insular network. NeuroImage 79:42–51.

Posner MI (2008) Measuring alertness. Ann N Y Acad Sci 1129:193–199.

Posner MI, Boies SJ (1971) Components of attention. Psychol Rev 78:391–408.

Power JD, Barnes KA, Snyder AZ, Schlaggar BL, Petersen SE (2012) Spurious but systematic correlations in functional connectivity MRI networks arise from subject motion. NeuroImage 59:2142–2154.

Reinvang I, Lundervold AJ, Rootwelt H, Wehling E, Espeseth T (2009) Individual variation in a cholinergic receptor gene modulates attention. Neurosci Lett 453:131–134.

Robertson IH, Garavan H (2004) Vigilant Attention. In: The Cognitive Neurosciences, 3rd ed., pp 563–578. Cambridge, MA: MIT Press.

Rubia K, Smith AB, Brammer MJ, Toone B, Taylor E (2005) Abnormal Brain Activation During Inhibition and Error Detection in Medication-Naive Adolescents With ADHD. Am J Psychiatry 162:1067–1075.

Sadaghiani S, D'Esposito M (2015) Functional Characterization of the Cingulo-Opercular Network in the Maintenance of Tonic Alertness. Cereb Cortex 25:2763–2773.

Sadaghiani S, Scheeringa R, Lehongre K, Morillon B, Giraud A-L, Kleinschmidt A (2010) Intrinsic Connectivity Networks, Alpha Oscillations, and Tonic Alertness: A Simultaneous Electroencephalography/Functional Magnetic Resonance Imaging Study. J Neurosci 30:10243–10250.

Sahgal A (1987) Some limitations of indices derived from signal detection theory: evaluation of an alternative index for measuring bias in memory tasks. Psychopharmacology (Berl) 91:517–520.

Sarter M, Paolone G (2011) Deficits in Attentional Control: Cholinergic Mechanisms and Circuitry-Based Treatment Approaches. Behav Neurosci 125:825–835.

Satterthwaite TD, Connolly JJ, Ruparel K, Calkins ME, Jackson C, Elliott MA, Roalf DR, Ryan Hopson KP, Behr M, Qiu H, Mentch FD, Chiavacci R, Sleiman PMA, Gur RC, Hakonarson H, Gur RE (2016) The Philadelphia Neurodevelopmental Cohort: A publicly available resource for the study of normal and abnormal brain development in youth. NeuroImage Available at: http://www.sciencedirect.com/science/article/pii/S1053811915002529 [Accessed July 27, 2015].

Satterthwaite TD, Elliott MA, Gerraty RT, Ruparel K, Loughead J, Calkins ME, Eickhoff SB, Hakonarson H, Gur RC, Gur RE, Wolf DH (2013) An improved framework for confound regression and filtering for control of motion artifact in the preprocessing of resting-state functional connectivity data. NeuroImage 64:240–256.

857 Satterthwaite TD, Elliott MA, Ruparel K, Loughead J, Prabhakaran K, Calkins ME, Hopson R,
858 Jackson C, Keefe J, Riley M, Mensh FD, Sleiman P, Verma R, Davatzikos C,
859 Hakonarson H, Gur RC, Gur RE (2014) Neuroimaging of the Philadelphia
860 Neurodevelopmental Cohort. NeuroImage 86:544–553.

861 Schumann G et al. (2010) The IMAGEN study: reinforcement-related behaviour in normal brain
862 function and psychopathology. Mol Psychiatry 15:1128–1139.

863 Seeley WW, Menon V, Schatzberg AF, Keller J, Glover GH, Kenna H, Reiss AL, Greicius MD
864 (2007) Dissociable intrinsic connectivity networks for salience processing and executive
865 control. J Neurosci 27:2349–2356.

866 Shirer WR, Ryali S, Rykhlevskaia E, Menon V, Greicius MD (2012) Decoding Subject-Driven
867 Cognitive States with Whole-Brain Connectivity Patterns. Cereb Cortex 22:158–165.

868 Störmer VS, Passow S, Biesenack J, Li S-C (2012) Dopaminergic and cholinergic modulations
869 of visual-spatial attention and working memory: Insights from molecular genetic research
870 and implications for adult cognitive development. Dev Psychol 48:875–889.

871 Sturm W, Longoni F, Fimm B, Dietrich T, Weis S, Kemna S, Herzog H, Willmes K (2004)
872 Network for auditory intrinsic alertness: a PET study. Neuropsychologia 42:563–568.

873 Tanner JM (1978) Growth at Adolescence, 2nd ed. Springfield, IL: Blackwell Science Ltd.

874 The 1000 Genomes Project Consortium (2015) A global reference for human genetic variation.
875 Nature 526:68–74.

876 The GTEx Consortium (2015) The Genotype-Tissue Expression (GTEx) pilot analysis:
877 Multitissue gene regulation in humans. Science 348:648–660.

878 Whelan R et al. (2012) Adolescent impulsivity phenotypes characterized by distinct brain
879 networks. Nat Neurosci 15:920–925.

880 Winterer G, Musso F, Konrad A, Vucurevic G, Stoeter P, Sander T, Gallinat J (2007)
881 Association of attentional network function with exon 5 variations of the CHRNA4 gene.
882 Hum Mol Genet 16:2165–2174.

883 Yeo BTT, Krienen FM, Eickhoff SB, Yaakub SN, Fox PT, Buckner RL, Asplund CL, Chee
884 MWL (2014) Functional Specialization and Flexibility in Human Association Cortex.
885 Cereb Cortex:bhu217.

886

Table 1: Demographics and genotype breakdown of included subjects

	IMAGEN cohort		PNC cohort	
	fMRI	**Behavioral**	**fMRI**	**Behavioral**
T/T carriers	354 (189 females)	403 (209 females)	66 (37 females)	608 (333 females)
T/C carriers	671 (340 females)	751 (383 females)	111 (55 females)	1077 (573 females)
C/C carriers	333 (166 females)	345 (168 females)	51 (25 females)	466 (250 females)
Total	1358 (695 females)	1499 (760 females)	228 (117 females)	2151 (1156 females)
Age (years)	14±0	14±0	16.9±1.8	16.7±1.9

Table 2: Contrasting task-evoked activity between T/C carriers and homozygotes

	MNI x y z coordinates	Peak t_{1344}	Peak *p*	Cluster size (voxels)	Corrected cluster *p**
CO Network					
Anterior insula - Right	36 20 -5	4.22	$<5*10^{-5}$	95	0.0004
- Left	-45 11 -2	4.16	$<5*10^{-5}$	54	0.002
- Left	-33 17 -8	4.52	$<5*10^{-5}$	14	0.040
Anterior prefrontal - Right	30 47 19	3.52	$<5*10^{-4}$	14	0.040
- Left	-30 50 7	4.50	$<5*10^{-5}$	22	0.017
Dorsal anterior cingulate - Left	-6 23 31	3.50	$<5*10^{-4}$	13	0.046
Non-CO regions					
Precentral gyrus - Left	-51 -10 40	4.0	$<5*10^{-5}$	38	0.005
- Right	33 -25 49	4.43	$<5*10^{-5}$	19	0.023
- Right, inferior	57 -1 24	3.81	$<5*10^{-4}$	17	0.028
Cuneus - Right	18 -78 31	3.68	$<5*10^{-4}$	30	0.010
Lingual gyrus - Left	-18 -49 4	4.16	$<5*10^{-5}$	28	0.010
Putamen - Left	-21 8 4	3.83	$<5*10^{-4}$	20	0.021
Superior temporal gyrus - Left	-66 -37 17	3.83	$<5*10^{-4}$	18	0.025

* Permutation-based, following an auxiliary uncorrected threshold p<0.005

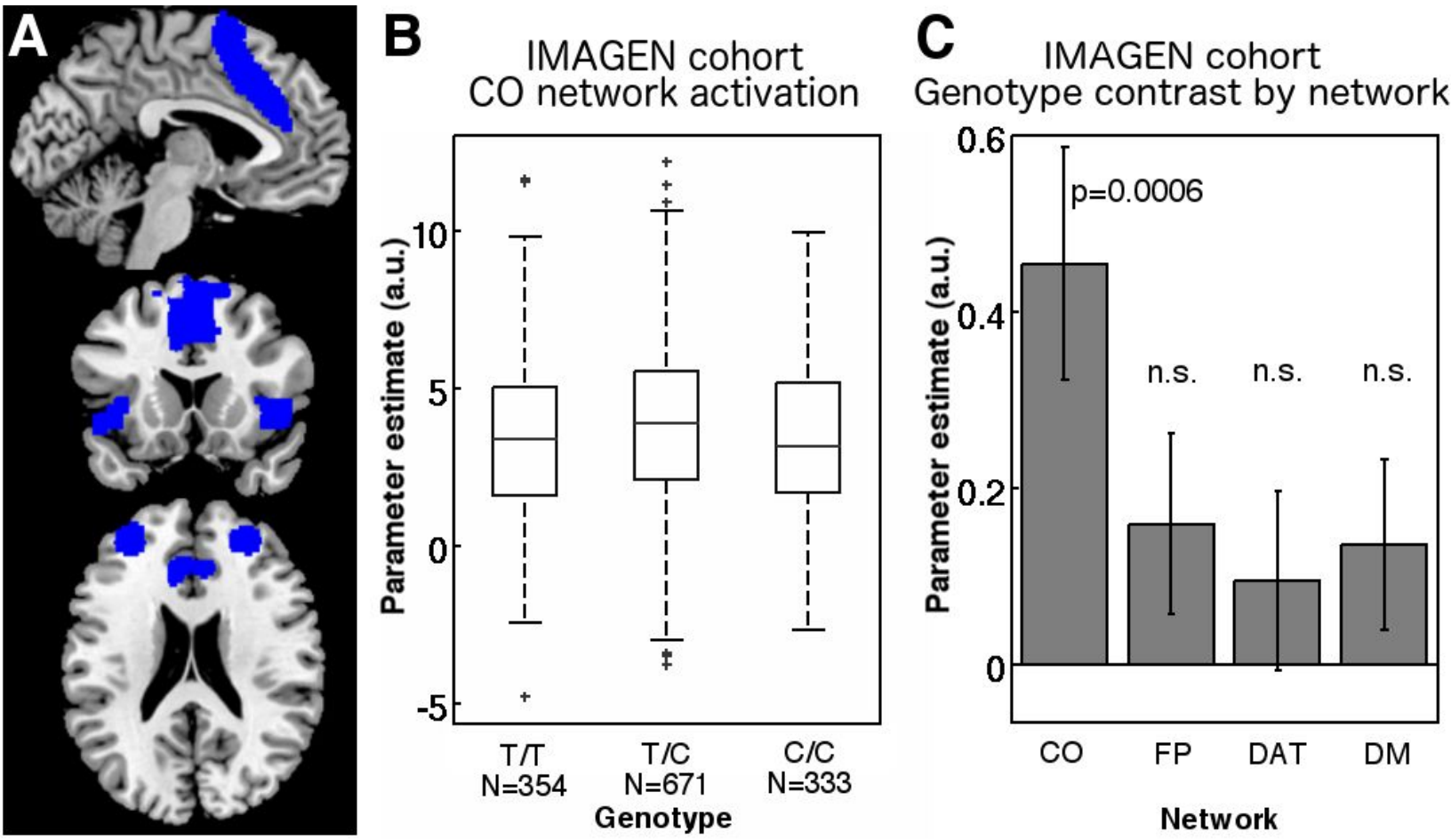
A
B
IMAGEN cohort
CO network activation
Parameter estimate (a.u.)
10
5
0
-5
T/T
N=354
T/C
N=671
C/C
N=333
Genotype
C
IMAGEN cohort
Genotype contrast by network
0.6
0.4
0.2
0
p=0.0006
n.s.
n.s.
n.s.
CO
FP
DAT
DM
Network

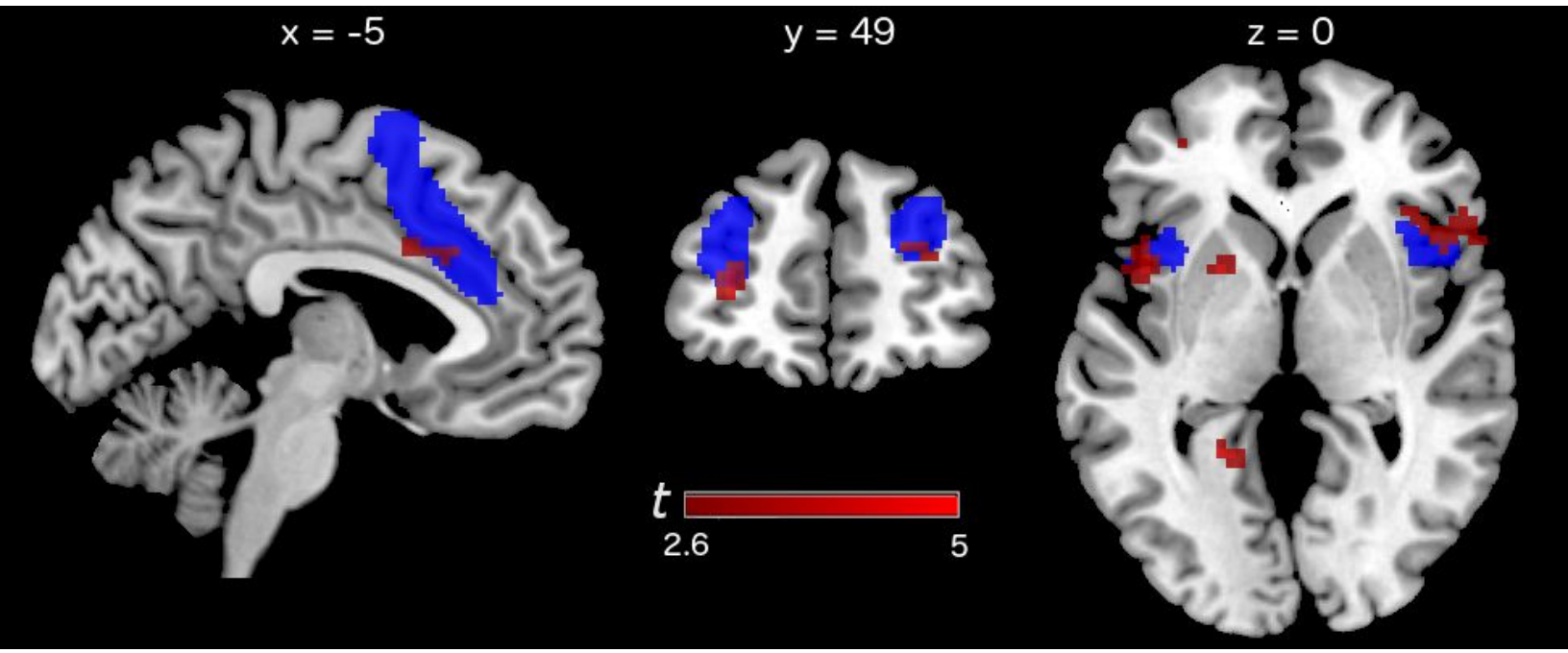
x = -5
y = 49
z = 0
t
2.6
5

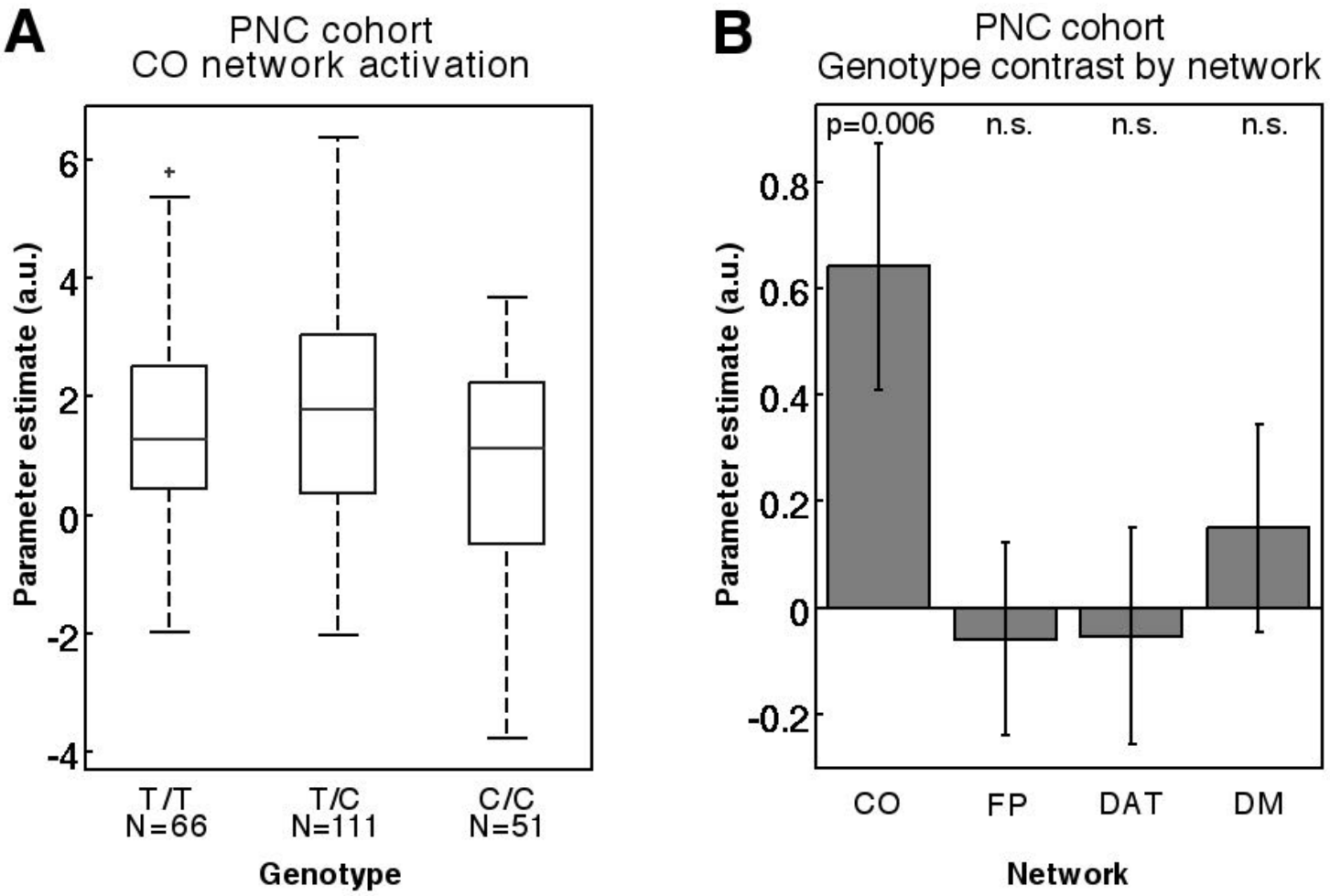
A
PNC cohort
CO network activation
Parameter estimate (a.u.)
6
4
2
0
-2
-4
T/T
N=66
T/C
N=111
C/C
N=51
Genotype
B
PNC cohort
Genotype contrast by network
p=0.006
n.s.
n.s.
n.s.
Parameter estimate (a.u.)
0.8
0.6
0.4
0.2
0
-0.2
CO
FP
DAT
DM
Network

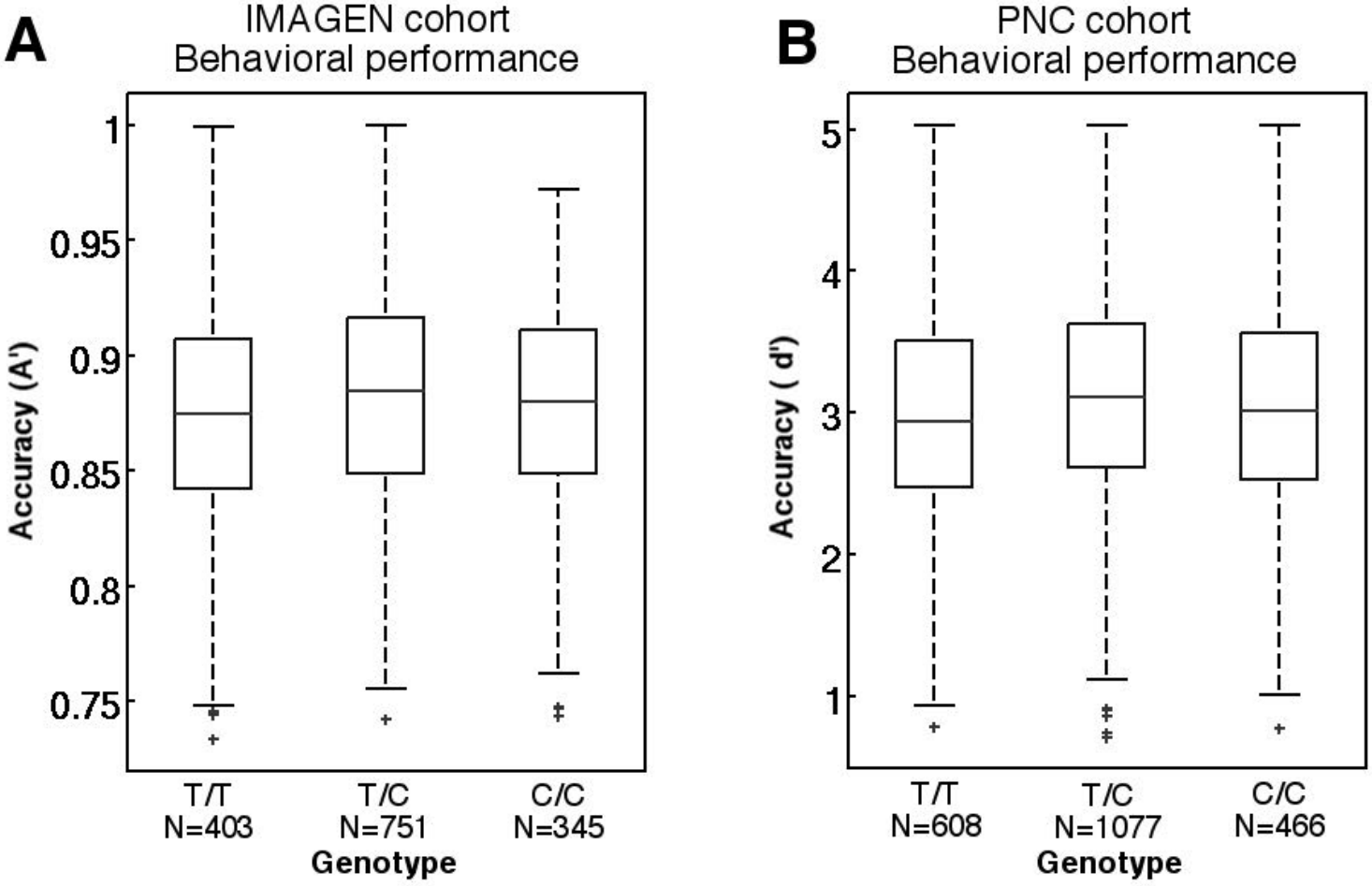
A
IMAGEN cohort
Behavioral performance
Accuracy (A')
1
0.95
0.9
0.85
0.8
0.75
T/T
N=403
T/C
N=751
C/C
N=345
Genotype
B
PNC cohort
Behavioral performance
Accuracy (d')
5
4
3
2
1
T/T
N=608
T/C
N=1077
C/C
N=466
Genotype